J. theor. Biol. (1999) **200,** 1–17
Article No. jtbi.1999.0972, available online at http://www.idealibrary.com on IDEAL®

The Biphasic Mystery: Why a Biphasic Shock is More Effective than a Monophasic Shock for Defibrillation

J. P. KEENER* AND T. J. LEWIS

Department of Mathematics, University of Utah, Salt Lake City, UT 84112, *U.S.A.*

(*Received on* 8 *April* 1999, *Accepted in revised form on* 19 *May* 1999)

We demonstrate that a biphasic shock is more effective than a monophasic shock at eliminating reentrant electrical activity in an ionic model of cardiac ventricular electrical activity. This effectiveness results from early hyperpolarization that enhances the recovery of sodium inactivation, thereby enabling earlier activation of recovering cells. The effect can be seen easily in a model of a single cell and also in a cable model with a ring of excitable cells. Finally, we demonstrate the phenomenon in a two-dimensional model of cardiac tissue.

1. Introduction

Although defibrillation by the application of large current shocks is accomplished daily in clinics and hospitals around the world, there is no adequate theoretical explanation for how defibrillation works. It is generally accepted that for successful defibrillation (about) 90% of cardiac tissue must experience an extracellular electric field of 5 V cm^{-1} for 10 ms (Zhou *et al.*, 1993a). However, it is not understood how tissue properties give rise to this defibrillation threshold quantity or how it might be decreased. Furthermore, the mechanism by which this extracellular electric field affects the transmembrane potential of individual cells is not completely resolved. Thus, there are several fundamental questions that must be answered to arrive at a comprehensive theoretical understanding of defibrillation. First, how can a spatially localized stimulus have a global effect on the transmembrane potential, and thereby affect the activation pattern far from the stimulating electrodes? Second, what are the dynamics of the medium subsequent to the application of a large shock that lead to the elimination of reentrant activation patterns? And finally, what is the most efficient way (stimulus protocol) to escort cardiac tissue through this trajectory?

In recent years, a theory of defibrillation has begun to emerge (Biktashev & Holden, 1998; Biktashev *et al.*, 1997; Holden, 1997; Keener, 1996, 1998; Keener & Panfilov, 1996; Krinsky & Pumir, 1998; Pumir & Krinsky, 1996, 1997). Although it is yet to be satisfactorily confirmed by experimental studies, this theory is promising, because it appears to answer some of the above fundamental questions.

This emerging theory is based on the "local resistive inhomogeneity hypothesis". According to this theory, resistive inhomogeneities on the microscopic space scale of cells create small transmembrane currents in every cell. These currents hyperpolarize the cell membrane at one end of the cell and depolarize the cell membrane at the other end, giving rise to a microscopic "sawtooth" variation in transmembrane potential,

*Author to whom correspondence should be addressed.
E-mail: keener@math.utah.edu.

0022–5193/99/017001 + 17 $30.00/0

which is superimposed on the variation on the macroscopic space scale of the tissue. If the amplitude of the cellular variation in transmembrane potential remains small, there is little net effect. However, when the applied field is large, the amplitude of these sawtooth variations can become adequate to invoke nonlinear effects of ionic currents and activate cells. That is, the effect of depolarization on one side of the cell can overcome the effect of hyperpolarization on the other side of the cell and lead to a net activation of the entire cell. The criteria for cell activation include the refractory state of the cell and stimulus properties such as amplitude, duration and waveform. The local resistive inhomogeneity hypothesis therefore gives a plausible explanation for direct field activation and a plausible answer to our first question.

Defibrillation is more difficult to accomplish than direct field activation. During fibrillation, cells are presumed to be in highly dispersed states of activity as a result of reentrant waves. To defibrillate, a shock must be effective regardless of the details of this physical distribution of states. One can imagine several ways to accomplish defibrillation in a general excitable medium (Pumir & Krinsky, 1997), but the scenario that appears to be at work in cardiac tissue relies on the following recovery property. Following a wave of excitation, there exists a minimal recovery time below which the tissue is in a recovery state such that it cannot support propagated wavefronts. Instead, any distortion in transmembrane potential caused by a stimulus acts like a waveback and it collapses in on itself. The idea for a successful defibrillatory stimulus is to excite all recovered and partially refractory media, thus effectively pushing all wavefronts into regions of tissue that are in recovery states that do not support propagation. This converts all action potential wavefronts into wavebacks, so that the waves regress rather than advance, and eventually collapse. This scenario is readily seen in numerical studies of two-dimensional tissue (Keener & Panfilov, 1996; Pumir *et al*., 1998). Thus, the theory is at a stage where the second fundamental question is being addressed quantitatively.

Here, we take the above explanations as the primary working hypotheses of this paper. Specifically, we assume that local resistive inhomogeneities create hyperpolarizing and depolarizing transmembrane currents in all cardiac cells and that the goal of these is to excite as much tissue as possible, thereby converting action potential wavefronts into wavebacks of recovery incapable of spreading, leading to a collapse of reentrant wave activity. With this in hand, we can begin to address our third fundamental question: what stimulus protocols are most efficient at accomplishing the above goal of defibrillation, and what are the ionic mechanisms making them most successful?

It is known from experimental studies that a biphasic shock is more efficient than a monophasic shock for defibrillation (Zhou *et al*., 1993a, b). To date, there has been no satisfactory theoretical explanation of this phenomenon. One recent study (Fishler *et al*., 1996b) found evidence for this phenomenon in a numerical simulation of a one-dimensional chain of cells with large gap junctional resistance as the source of local resistive inhomogeneity. However, an adequate explanation of the phenomena in terms of ionic mechanisms is not provided there, nor is it apparent how to examine the response of stimuli in two or three dimensional tissue domains, capable of self-sustained fibrillatory wave patterns.

The leading hypothesis for this improvement, first suggested in Jones *et al*. (1987), is that the first phase of the bipolar waveform acts as a conditioning pre-pulse that enhances or reestablishes sodium current excitability, thereby reducing the activation threshold for the second phase of the waveform, and leads to improved responsiveness. However, this early investigation studied the effect of direct current injection into single cells, and is therefore not *directly* applicable to defibrillation (because it does not address the question of how cells can receive the appropriate stimulus from electrodes that are many space constants away). More recently, several studies have found similar behavior in single cells stimulated via an extracellular field (Fishler *et al*., 1996a; Jones *et al*., 1994; Leon & Roberge, 1993; Tung & Borderies, 1992), giving further credence to this hypothesis. It remains to demonstrate that this is indeed the primary mechanism at work in annihilating reentrant activity, which is associated with fibrillation, in one-, two- and three-dimensional tissue.

The purpose of this paper is to demonstrate that biphasic shocks are usually more efficient than monophasic shocks at defibrillation, and to describe the ionic mechanism for this difference. In what follows, we describe a mathematical model for defibrillation, explore the effect of monophasic and biphasic stimuli on single cells, and then demonstrate the effect of these stimuli on one- and two-dimensional collections of cells. Indeed we demonstrate that, as suggested by single-cell studies, the first phase of the bipolar waveform acts as a conditioning prepulse that reestablishes sodium current excitability, thereby reducing the activation threshold for the second phase of the waveform. This is turn leads to an improved activation of partially refractory tissue and enables the wavefront to be pushed further into the refractory tail of the preceding action potential, leading to its eventual collapse.

2. A Model to Study Defibrillation

In this section, we summarize a model for the cell-averaged electrical activity in cardiac tissue that is used in the remainder of this paper. A detailed derivation of this model was given in Keener and Panfilov (1996) (see also Keener & Sneyd, 1998). It can be assumed that cardiac tissue is divided between intracellular space and extracellular space; however it is impractical to keep track of the details of these separate spaces. Fortunately, the smallness of the cells relative to the macroscopic electrical length constant can be exploited in order to obtain averaged equations. These equations come in the form of the classical bidomain model (Plonsey, 1988) in which it is assumed that cardiac tissue is a two-phase medium at the macroscopic level with comingled intracellular and extracellular domains. At each point of the cardiac domain, there are mean potentials ϕ_e and ϕ_i, the extracellular and intracellular potentials, respectively, and the transmembrane potential, $V = \phi_i - \phi_e$. These potentials drive currents,

$$i_e = -\sigma_e \nabla\phi_e, \qquad i_i = -\sigma_i \nabla\phi_i, \tag{1}$$

and a transmembrane current across the cell membrane that divides the two (comingled) regions. The conductivities of the two domains are represented by the conductivity tensors, σ_i and σ_e, which represent average, or effective, conductances of the media. Since current is conserved, Kirchhof's laws imply that

$$\chi\left(C_m \frac{\partial V}{\partial t} + I_{ion}\right) = \nabla \cdot (\sigma_i \nabla\phi_i), \tag{2}$$

$$\nabla \cdot (\sigma_i \nabla\phi_i + \sigma_e \nabla\phi_e) = 0. \tag{3}$$

Equation (2) implies that current can leave the intracellular space only as a transmembrane current, and that the transmembrane current has two components, namely the capacitive current and the ionic current I_{ion}. Equation (3) states that the total of intracellular and extracellular current $I_{tot} = -\sigma_i \nabla\phi_i - \sigma_e \nabla\phi_e$ is conserved, since there are no intracardiac current sources. In eqn (2), C_m is the membrane capacitance, and χ is the surface to volume ratio of the cell. In the case of one spatial dimension or when the intracellular and extracellular conductivities have an equal anisotropy ratio, eqns (2) and (3) can be reduced to a single equation

$$\chi\left(C_m \frac{\partial V}{\partial t} + I_{ion}\right) = \nabla \cdot (\sigma \nabla V), \tag{4}$$

where $\sigma = \sigma_i(\sigma_i + \sigma_e)^{-1}\sigma_e$ is the effective conductivity (tensor) for the medium.

Generally, the ionic currents are represented as

$$I_{ion} = f(V, w), \tag{5}$$

where w represents other variables such as gating variables, and follow dynamics of the form

$$w_t = g(V, w), \tag{6}$$

a system of ordinary differential equations.

When a large field is applied to the medium, it is not sufficient to know only the mean field, because the effect of resistive inhomogeneities becomes important and the microstructure of the medium must be taken into account. It is shown in Keener and Panfilov (1996) that the microstructural intracellular and extracellular

potentials can be represented by

$$\psi_i = \phi_i(x) + \varepsilon W_i(z) \cdot T^{-1}(x) \nabla \phi_i(x), \quad (7)$$

$$\psi_e = \phi_e(x) + \varepsilon W_e(z) \cdot T^{-1}(x) \nabla \phi_e(x). \quad (8)$$

The variable x is the three-dimensional spatial Cartesian coordinate for the cardiac domain, and $z = x/\varepsilon$ is a "fast" three-dimensional spatial variable, on the scale of cells. The number ε is the ratio of cell length to longitudinal space constant $\varepsilon = l/\Lambda$, and is generally small, on the order of 0.1–0.2. The vector-valued functions $W_i(z)$ and $W_e(z)$, which reflect the details of cellular structure, are periodic in z and have zero mean value. The possibility of variable orientation of the cells is reflected in the x dependence of the rotation matrix $T(x)$, whose rows are the normalized orthogonal axes of the cell. Further, the transmembrane potential, $\psi = \psi_e - \psi_i$, becomes

$$\psi = V(x) + \varepsilon H(z, x), \quad (9)$$

where $H(z, x) = W_i(z) \cdot T^{-1}(x) \nabla \phi_i - W_e(z) \cdot T^{-1}(x) \nabla \phi_e$. In the case of one spatial dimension with the intracellular conductance idealized as a constant base level plus delta function jumps (representing gap junctions) and the extracellular conductance approximated by a constant, $W_e = 0$ and $W_i = -\beta[z \,(\mathrm{mod}\, 1) - \frac{1}{2}]$, where β is a constant involving a combination of the conductivities of the gap junction and the intracellular and extracellular fluid. Notice that W_i, and thus H, accounts for the sawtooth variation in potentials mentioned earlier.

These modifications of the electrical potential average to zero over the length of the cell everywhere in eqns (2) and (3) except in the ionic current term (the only nonlinear term). Therefore, the ionic current used in eqn (2) must be taken to be

$$I_{ion} = \frac{1}{S} \int_{\partial\Omega} f(V + \varepsilon H(z, x), w(x, z))\, \mathrm{d}z, \quad (10)$$

i.e. the average of f with respect to the variable z over the surface of a single cell, $\partial\Omega$, with total surface area S. This modification of the transmembrane current is significant only when there is a large externally applied current, because large external stimuli lead to large (of the order ε^{-1}) $\nabla \phi_i$ and $\nabla \phi_e$ making the modification terms the same order as the mean potentials. With no such input, the contribution of rapidly varying terms is inconsequential and can be ignored, in which case eqn (10) reduces to the usual ionic current in eqn (5).

The dynamics of the gating variables w is also modified by the local spatial inhomogeneity to

$$w_t = g(V + \varepsilon H(z, x), w). \quad (11)$$

It is because of the z dependence of the right-hand side of this equation that w may also develop z dependence during the application of a large field.

The z dependence of w is problematic, because it is impossible (or certainly impractical) to follow in detail in a simulation of a large piece of tissue. Therefore, we replace the functions $W_i(z)$ and $W_e(z)$ by a simple piecewise constant approximations using two interpolation points z_- and z_+ with z_- in the left-half of the cell and z_+ in the right-half of the cell. [This is equivalent to a representation of $W_i(z)$ and $W_e(z)$ in terms of the orthogonal Walsh functions (Keener, 1988)]. With this simplification and the assumption that $W(z_-) = -W(z_+)$ (e.g. symmetric cells), the transmembrane potential becomes $V + A$ on half of the cell membrane and $V - A$ on the other half, where $A = \varepsilon W_i(z_+) T^{-1} \nabla \phi_i - \varepsilon W_e(z_+) T^{-1} \nabla \phi_e$, a function of x alone. While it is possible to determine A as part of the solution of the bidomain equations in response to boundary conditions with an applied current, for this paper, we simply take $A = \gamma I_0(t)$, where $I_0(t)$ is the externally applied current, and γ (independent of x) is some constant relating the applied current to the amplitude of the deflection of the transmembrane potential. The parameter γ depends in important ways on the nature of the tissue (Keener, 1998), but its actual numerical value is of little consequence to this study (provided it is not zero).

On the two different regions of cell membrane, there are two different values of the gating variables, governed by

$$w_t^{\pm} = g(V \pm A, w^{\pm}), \quad (12)$$

where w^+ are the gating variables on that region of the cell where $\psi = V + A$, and w^- are the gating variables on that region of the cell where $\psi = V - A$. With this simplification, the average ionic current (10) simplifies to

$$I_{ion} = \tfrac{1}{2}\,(f(V + A,\, w^+) + f(V - A,\, w^-)). \quad (13)$$

The version of the bidomain model that is studied in this paper consists of eqn (4) with ionic current specified by eqn (13) and gating variables governed by eqn (12). This model was originally derived by Biktashev *et al.* (1997).

The most important feature of this model (and principle difference from the models of defibrillation discussed in Keener (1996, 1998; Keener & Panfilov (1996), Krinsky & Pumir (1998 and Pumir & Krinsky 1996, 1997) is that it keeps track of the possible differences of the gating variables in different regions of a cell during the time that a stimulus is applied. It is precisely this feature that leads to differences in the effects of monophasic and biphasic stimuli, and the feature that is the subject of the discussion that follows. We emphasize that it is not necessary to numerically resolve this model at the spatial resolution of cells. Rather, this model represents a variation on the idea of the bidomain model, that at every point of physical space there are two potentials. Here, we are assuming that at every point of physical space there are two sets of gating variables, corresponding to the two sides (or compartments) of each cell, that must be tracked.

3. The Response of a Single Cell

Before discussing how defibrillation takes place and why a biphasic shock is more effective for defibrillation, it is necessary to understand the response of a single cell to stimuli.

Because current diffusion is rapid on the length scale of the cell, the diffusion term on the right-hand side in eqn (2) can be ignored for a single cell, hence the transmembrane potential for an isolated myocyte is governed by

$$C_m \frac{\partial V}{\partial t} = -I_{ion}. \quad (14)$$

In this and all remaining sections, we use the Beeler–Reuter model (Beeler & Reuter, 1977) to represent the ionic current of a cardiac myocyte, I_{ion}. The Beeler–Reuter model describes I_{ion} as the sum of four separate ionic currents: a sodium current, a time-independent and a time-activated potassium current and a calcium current. These currents are controlled by six gating variables, m, h, j, d, f and x_1, and the intracellular calcium concentration ($[Ca^{2+}]_i$), which are governed by ordinary differential equations. The equations for the gating variables are of the form

$$\frac{dw}{dt} = \frac{1}{\tau_w(V)}\,[w_\infty(V) - w]. \quad (15)$$

This equation implies that as the transmembrane potential, V, changes at a rate associated with the time constant, $C_m R_m$ (where R_m is the instantaneous membrane resistivity), w tracks V by moving toward its instantaneous steady-state value $w_\infty(V)$ with an instantaneous time constant $\tau_w(V)$.

For this discussion, the most important current is the sodium current, which is represented by

$$I_{Na} = (4m^3 hj + 0.003)\,(V - 50). \quad (16)$$

The product $m^3 hj$ can be thought of as the fraction of the time-dependent sodium current that is recruited. The variable m is a fast activation variable. It increases with depolarization of the membrane and its associated time constant is small enough to keep m quite close to its steady-state value $m_\infty(V)$. The variables h and j are inactivation variables, because their steady-state values decrease when the membrane is depolarized. The variable h represents "fast" sodium current inactivation (although h is slower than m) and j represents "slow" inactivation (although it is generally faster than other gating variables, i.e. d, f, x_1). Figure 1 depicts the time constants and steady-state value of m, h and j as a function of V. It should be noted that there is disagreement in the literature about the necessity of the slow inactivation variable j. For example, the Ebihara-Johnson model (Ebihara & Johnson, 1980) does not include j, while the Luo–Rudy model (Luo & Rudy, 1994a, b) does. Some recent

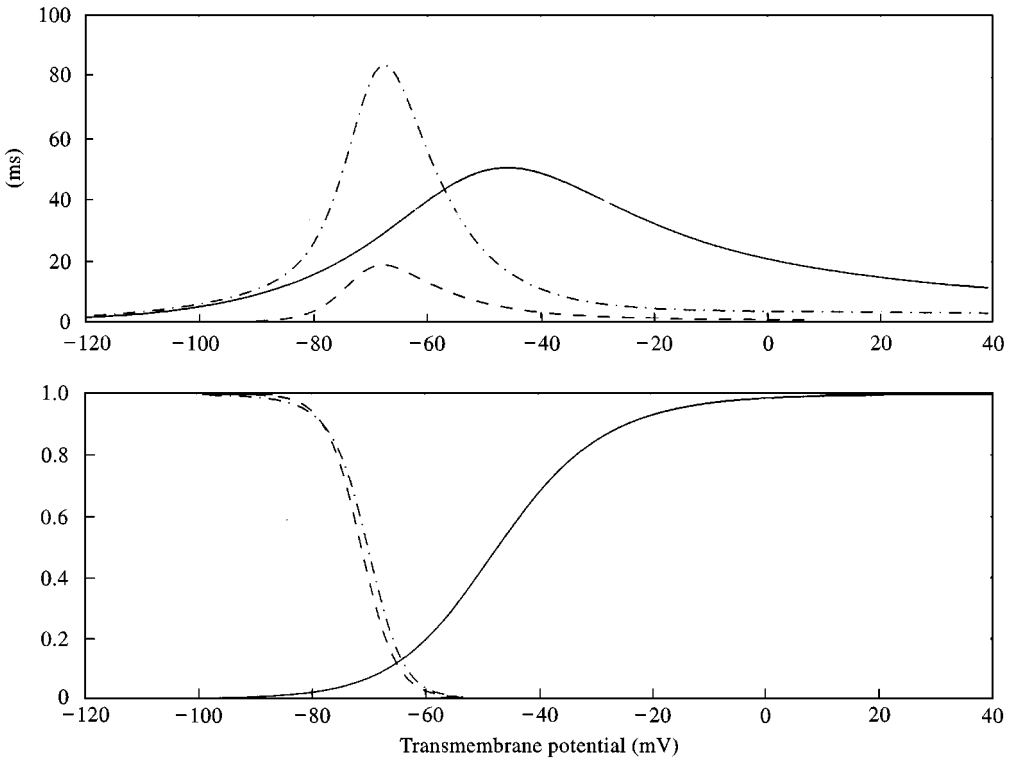

FIG. 1. The time constants (top) and the steady-state values (bottom) of m, h, and j as functions of transmembrane potential. m_∞ (——); h_∞ (- - - -); j_∞ (– · – · –).

data suggests that the slow inactivation has a typical time constant on the order of seconds (Richmond *et al.*, 1998), which is far too slow to have an effect on defibrillatory processes lasting only 10 ms.

To understand the response of a single cell to an extracellular stimulus, it is valuable to first review the simpler scenario of the response of a cell to an applied intracellular current. It is well known that if the applied inward current is of small amplitude and duration, the membrane acts as a capacitor and depolarizes, but the membrane potential quickly returns to rest after the stimulus ends. On the other hand, if the stimulus has sufficient amplitude and duration, then the initial capacitive depolarization brings V to a threshold potential and triggers the autocatalytic activation of the sodium current. This further depolarizes the membrane potential and generates the rapid upstroke of an action potential. It is important that the depolarizing stimulus be both sufficiently large and rapid. This is because, besides activating the sodium current (increasing m), depolarization also has the effect of increasing the sodium current inactivation (decreasing h and j). If the stimulus is large and rapid, the membrane depolarizes rapidly to threshold and activates the sodium current rapidly, before h and j can substantially change. However, if the stimulus is longer but of smaller amplitude, then the membrane potential changes more slowly and the inactivation variables can decrease substantially therefore shutting off the sodium current ($m^3 hj \approx 0$) before an action potential upstroke can be evoked.

One of the ways that the activation threshold is controlled is through the level of sodium current inactivation at the beginning of the depolarizing stimulus. In particular, a hyperpolarizing prepulse has the effect of reducing inactivation (note that there is a non-zero resting level of inactivation) thereby temporarily lowering the threshold for action potential generation (Jones *et al.*, 1987). This is the key to understanding the increased efficacy of a biphasic extracellular stimulus over a monophasic one.

A cell that is stimulated via an extracellular field experiences depolarization at one side of the

cell and hyperpolarization at the other (Fishler *et al.*, 1996b; Knisely *et al.*, 1993; Leon & Roberge, 1993; Pumir *et al.*, 1998; Tung & Borderies, 1992). If the depolarization at the one side of the cell is sufficient in amplitude and duration to activate the sodium current, the entire cell will be depolarized after the stimulus is removed. (Note that the current generated at this side of the cell must overcome the hyperpolarizing current at the other side of the cell due to the stimulus. However, also note that ionic currents recruited on the hyperpolarized side are inward/depolarizing). The hyperpolarized side of the cell is also affected in an important way, because the level of inactivation can be significantly reduced. This renders the hyperpolarized side of the cell more excitable. Thus, if the depolarization alone is of insufficient strength and duration to excite the cell, it may be that the cell can be excited by reversing polarity in the middle of the stimulus, thereby activating the cell through ionic current generated at the side that was previously hyperpolarized.

It is precisely this "facilitation" mechanism that explains why a biphasic stimulus is sometimes effective when a monophasic stimulus is not. A monophasic stimulus is successful if it is able to activate enough of the sodium current on the depolarized side to depolarize the entire cell. A biphasic stimulus is successful because the activation threshold is lowered at the side of the cell that is first hyperpolarized, and thus the sodium current is more easily activated when the polarity of the stimulus is reversed and that particular side is depolarized.

We can see how this works in numerical simulations of the Beeler–Reuter dynamics (although all ionic models with sodium activation and inactivation should have similar responses). In these simulations, I_{ion} is determined using the two-point-averaged ionic current (13), and the gating variables are specified by eqn (12). Specifically, this means that there are two copies of each of the gating variables, one copy for the side of the cell that is initially depolarized by the stimulus and one copy for the side of the cell that is initially hyperpolarized by the stimulus. [A two-point discretization is the simplest possible discretization that shows these effects. Other authors have used higher-resolution discretizations—from 3 points in Tung & Borderies (1992) and 11 points in Fishler *et al.* (1996b) to 48 in Leon & Roberge (1993)—but the results are qualitatively unchanged].

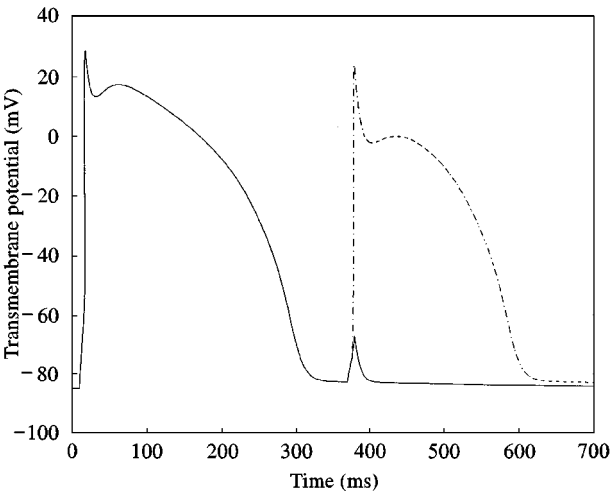

FIG. 2. Transmembrane potential for a single Beeler–Reuter cell subject to monophasic and biphasic field stimuli. Each stimulus amplitude (A) is 17.0 mV, duration is 10 ms and is applied 360 ms after the initial action potential. The solid curve represents response of the cell to a monophasic stimulus and the dashed-dotted curve shows the response of the cell to a biphasic stimulus. Notice that for a stimulus of the same amplitude, duration and timing, the biphasic stimulus is successful at activating the cell, whereas the monophasic stimulus fails to activate the cell. Monophasic (——); biphasic (– · – · –).

Figure 2 shows the change in transmembrane potential as the result of monophasic and biphasic extracellular stimuli. The first action potential in the sequence is the result of a superthreshold intracellular stimulus delivered to a resting cell at time $t = 10$ ms. The subsequent extracellular stimulus, taking $A = 17.0$ mV for a duration of 10 ms, was applied at time $t = 370$ ms (coupling interval 360 ms). The monophasic stimulus was unsuccessful in evoking an action potential (response shown as a solid curve), whereas the biphasic stimulus was successful (response shown as a dash-dot line). The polarity of the biphasic stimulus was switched at 5 ms.

The details of the gating variables during the application of the stimulus can be seen in Fig. 3. The top subfigure in Fig. 3 shows the transmembrane potential from Fig. 2 on a shorter time window in which the effect of the stimulus can be seen more easily. In the bottom three subfigures

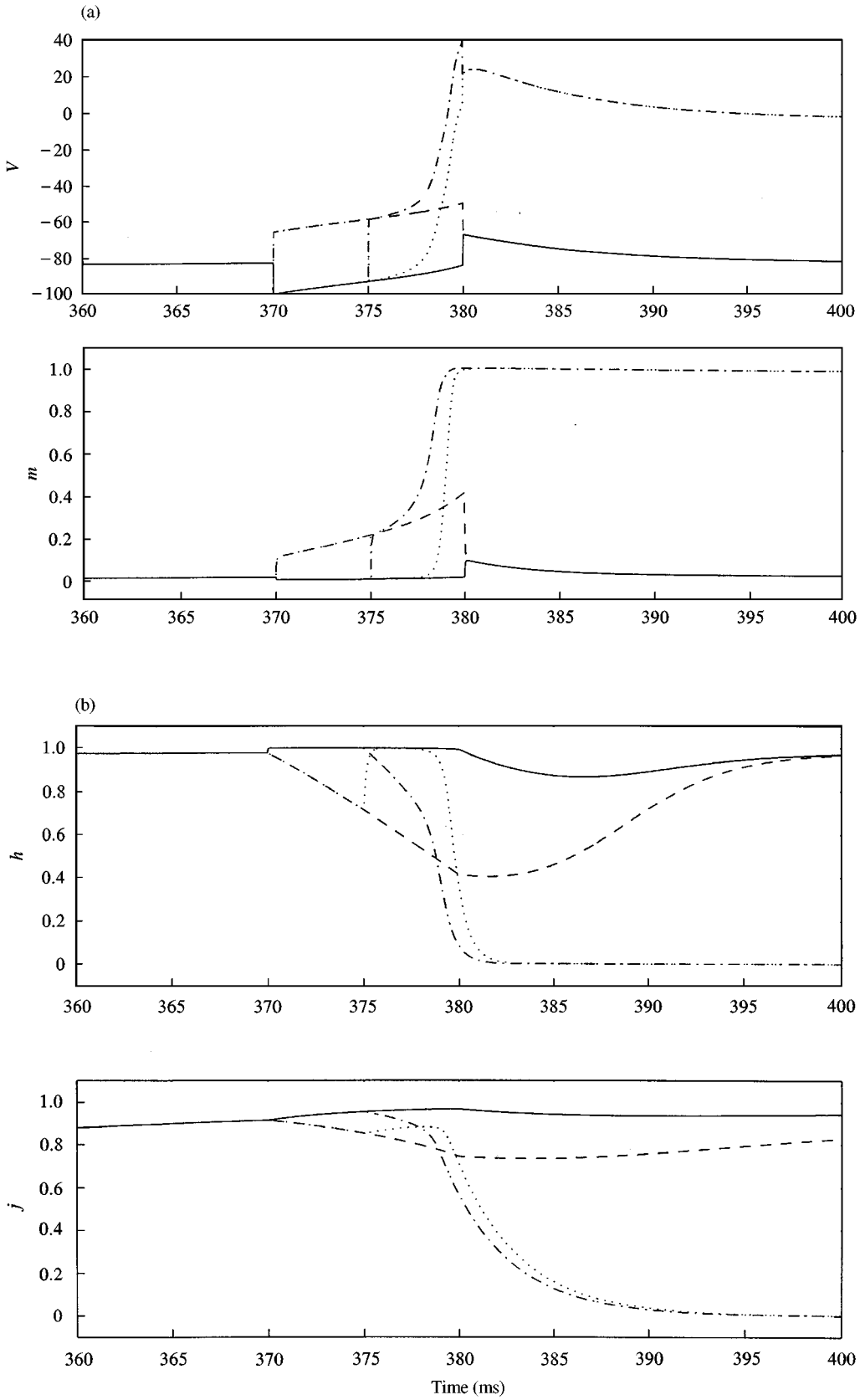

FIG. 3. Legend opposite.

in Fig. 3, the corresponding gating variables m, h, and j are shown. In each of these figures there are four curves, two representing the response to a monophasic stimulus and two for a biphasic stimulus. The curves labeled "+" correspond to dynamics in that part of the cell that is initially depolarized (with $V+A$) and similarly, curves labeled "−" correspond to dynamics in that part of the cell that is initially hyperpolarized (with $V-A$). For the monophasic stimulus, the "+" side remains relatively depolarized and the "−" side remains relatively hyperpolarized throughout the stimulus, but for the biphasic stimulus, the "+" side becomes relatively hyperpolarized and the "−" side becomes relatively depolarized after the polarity of the stimulus is reversed. Prior to the stimulus, monophasic and biphasic, as well as "+" and "−", curves are identical. During the first half of the stimulus interval, "+" and "−" curves diverge, however, the monophasic and biphasic curves remain identical. Once the polarity flips during the biphasic stimulus, the monophasic and biphasic curves diverge.

The m curves show the difference in transmembrane potential response but do not show the reason for the difference. As expected, m is depressed in the hyperpolarized part of the cell and elevated in the depolarized part of the cell. For the monophasic stimulus, the depolarization is insufficient to activate the cell, but for the biphasic stimulus, the cell is activated almost immediately following reversal of the stimulus polarity.

The h and j curves are much more revealing of the mechanism underlying this difference. As expected, both h and j are reduced (hence inactivated) by depolarization and increased (hence inactivation is reduced) by hyperpolarization. With the monophasic stimulus, the depolarization cannot activate the cell, because the depolarization cannot increase m rapidly enough to overcome the decrease in h and j. The biphasic stimulus, in contrast, exploits the effect of hyperpolarization by activating the sodium current on the side of the cell that was initially hyperpolarization and thereby rendered more excitable.

The behavior of all remaining variables shows no significant difference between the depolarized and hyperpolarized sides (not shown here). The reason for this is that either the variables are too slow to significantly respond directly to the 10 ms stimulus of the particular amplitude given here (x_1, f), the steady-state value does not change significantly in the interval of transmembrane potential that is important here (d), or the variable directly or indirectly has no major effect on activation threshold ($[Ca^{2+}]_i$).

This difference between monophasic and biphasic stimuli is qualitatively similar but varies quantitatively for different parameter values. For example, the dependence of the activation threshold (in units of A) is shown in Fig. 4 plotted as a function of coupling interval. Notice that biphasic stimulation has a lower activation threshold than monophasic stimulation for all coupling intervals, but the difference increases drastically for the small coupling intervals (below about 325 ms). This is critical in the mechanism for defibrillation. The previous figures used a coupling interval of 360 ms, which is close to the minimal threshold for both stimulus protocols according to this plot.

The difference between monophasic and biphasic stimuli depends on the length of the stimulus. If the stimulus is of extremely short duration, there is insufficient time for the inactivation variables h and j to respond significantly to the hyperpolarizing pulse, and so there is no advantage for a biphasic stimulus. However, as the pulse

FIG. 3. The response of a single Beeler–Reuter cell subject to monophasic and biphasic field stimuli. The curves from top to bottom represent the transmembrane potential V, the activation variable m, the inactivation variable h, the inactivation variable j. The stimuli are as described in Fig. 1. Of the four curves in each subfigure, two correspond to the monophasic stimulus and two to the biphasic stimulus; Of the two curves for each type of stimulus, one is for the "+" side of the cell and one each for the "−" side of the cell. The mechanism for the increased effectiveness of the biphasic stimulus reveals itself in the dynamics of the sodium current inactivation variables h and j. Both h and j are reduced (hence inactivated) by depolarization and increased (hence inactivation is reduced) by hyperpolarization. With the monophasic stimulus, the depolarization cannot activate the cell, because the depolarization cannot increase m rapidly enough to overcome the decrease in h and j. The biphasic stimulus, in contrast, exploits the effect of hyperpolarization by activating the sodium current on the side of the cell that was initially hyperpolarized and thereby rendered more excitable. Mono− (——); mono+ (– – –); bi− (– · – · –); bi+ (· · · · ·).

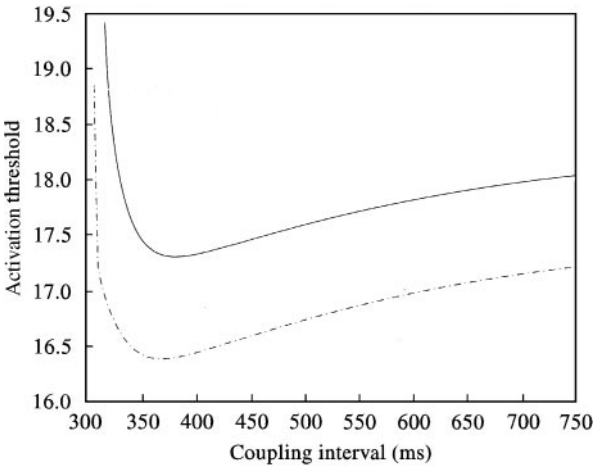

FIG. 4. Activation threshold A (in units of mV) plotted as a function of coupling interval for monophasic and biphasic stimuli of duration 10 ms. Notice that biphasic stimulation has a lower activation threshold than monophasic stimulation for all coupling intervals, but the difference increases drastically for the small coupling intervals (below about 325 ms). Monophasic (——); biphasic (– · – · –).

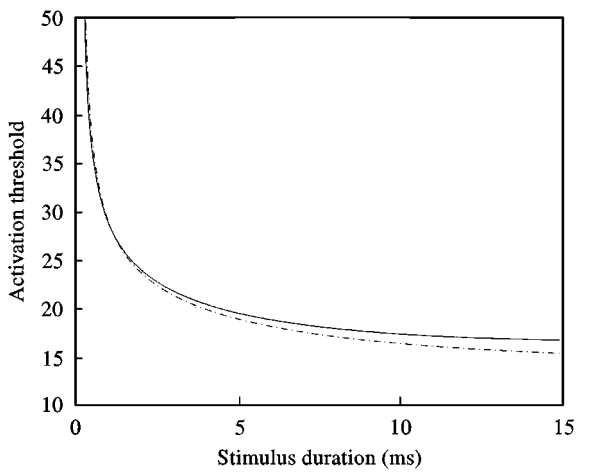

FIG. 5. Activation threshold A and mV plotted as a function of stimulus duration for monophasic and biphasic stimuli with fixed coupling interval 360 ms. The difference between monophasic and biphasic stimuli depends on the length of the stimulus. Only for stimuli of extremely short duration does a monophasic stimulus have a lower threshold than a biphasic stimulus. This is because there is insufficient time for the inactivation variables h and j to respond significantly to the hyperpolarizing pulse. Monophasic (——); biphasic (– · – · –).

duration is lengthened, the advantage of the biphasic stimulus increases. This increasing advantage can be seen in Fig. 5 where the activation threshold is plotted as a function of stimulus duration with fixed coupling interval 360 ms. For these parameter values, the two protocols have the same threshold at about 1 ms duration.

4. Elimination of Reentrant Patterns

To see if this phenomenon of single-cell behavior explains the mechanism of defibrillation, it is necessary to explore the response of spatially coupled cells. For this study, we simulated the Beeler–Reuter model equations on a ring of length 15.8 cm [i.e. eqn (4) with periodic boundary conditions]. The parameters were as follows: $C_m = 1\ \mu F$, $\chi = 5000\ \text{cm}^{-1}$, and $\bar{\sigma} = 0.005\ \Omega^{-1}\ \text{cm}^{-1}$ (average effective conductivity) (Courtemanche & Winfree, 1991). A mixed implicit–explicit half-step integration method (Hines, 1984) was used with a time-step of 0.02 ms and a space-step of 0.0063 cm and initial conditions were chosen in order to evoke a periodic wave rotating around the ring. The propagation velocity of this rotating pulse was $0.0479\ \text{cm ms}^{-1}$ and the action potential duration was 215 ms. At some arbitrary time after the periodic motion was well established, an extracellular stimulus of duration 10 ms was applied to the ring, and subsequent motion of the action potential observed.

The simulations show that A must be greater than 19.0 mV to eliminate the rotating wave with a monophasic stimulus, whereas to eliminate the wave with a biphasic stimulus, A need only be greater than 16.5 mV. Figures 6 and 7 show the behavior of the transmembrane potential immediately before, during and after the application of the shock of amplitude $A = 17.5$ mV with duration 10 ms. The monophasic shock, depicted in Fig. 6 is unsuccessful at eliminating the reentry, while the biphasic shock, depicted in Fig. 7 successfully eliminates the wave. In both cases, the shock has the effect of exciting the partially recovered medium directly ahead of the action potential, and hence the wavefront is effectively pushed ahead into less recovered medium that is closer to the tail of the "preceding" action potential. However, the difference between the two protocols is that the excited region is pushed further forward by the biphasic shock than by the monophasic shock. In fact, the monophasic shock pushes the wavefront into a region where it is slowed but not halted. The biphasic shock, on

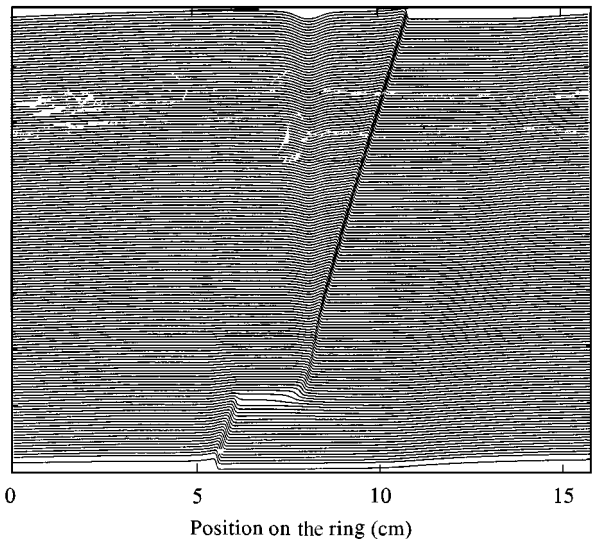

FIG. 6. The transmembrane potential V (mV) in a one-dimensional ring ($L = 15.8$ cm) of Beeler–Reuter tissue during and following the application of a monophasic stimulus of duration 10 ms and amplitude $A = 17.5$. Prestimulus dynamics correspond to a circulating pulse. Each curve is the solution at a fixed time and as time progresses the curves are lifted slightly. The output time step is 0.5 ms. The monophasic shock has the effect of exciting the partially recovered medium directly ahead of the action potential, and hence the wavefront is effectively pushed ahead into less recovered media that is closer to the tail of the "preceding" action potential. However, the monophasic shock pushes the wavefront into a region where it is slowed but not halted and the reentry persists.

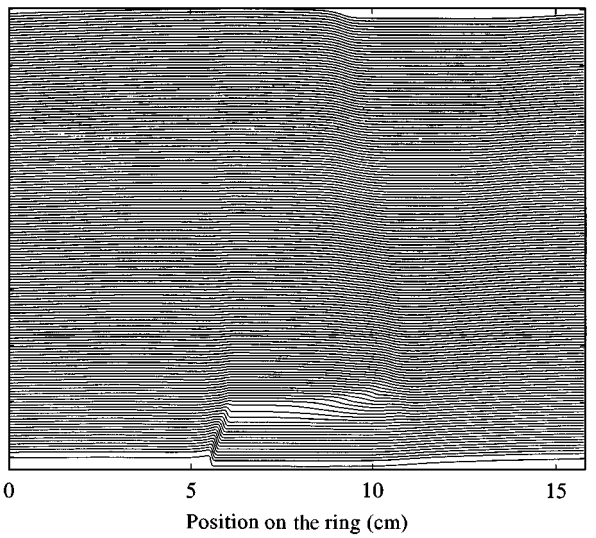

FIG. 7. The transmembrane potential V (mV) in a one-dimensional ring ($L = 15.8$ cm) of Beeler–Reuter tissue during and following the application of a biphasic stimulus. As in the simulation shown in the previous figure, the stimulus had a duration of 10 ms and an amplitude $A = 17.5$, and the prestimulus dynamics correspond to a circulating pulse. Each curve is the solution at a fixed time and as time progresses the curves are lifted slightly. The output time step is 0.5 ms. Again the shock has the effect of exciting the partially recovered medium directly ahead of the action potential, and hence the wavefront is effectively pushed ahead into less recovered media that is closer to the tail of the "preceding" action potential. However, the biphasic shock is able to activate media that is less recovered than the monophasic shock does. In fact, the wavefront is pushed so far forward that it is in a region that cannot support propagation. The result is that the wave collapses and the reentrant behavior is annihilated.

the other hand, is able to activate media that is less recovered and thus pushes the wavefront so far forward that it is in a region that cannot support propagation. As a result, the wave collapses and the reentrant behavior is annihilated.

The ionic mechanism underlying this difference is the same as seen in single-cell simulations. Figures 8 and 9 show the potential V and inactivation variables h and j as functions of time during and following the application of the stimulus, at two different positions on the ring. In Fig. 8, for position $x = 7.875$ cm, the medium is activated by the shock, but much more quickly with the biphasic shock than with the monophasic shock. As with single cells, the biphasic shock eliminates inactivation in the hyperpolarized portion of the cell with the first phase of the shock, and activates the cell when the polarity of the shock is reversed. At this position ($x = 7.875$ cm), the activation following the monophasic shock is due to propagation because it occurs after the new position of the wavefront is established following the termination of the shock.

At position $x = 9.450$ cm (see Fig. 9), the difference in response is more dramatic. Here, the monophasic shock has virtually no effect on the action potential, while the biphasic shock produces direct activation. The mechanism for this difference is similar to that described previously for the response of a single cell. The important difference, however, is that following the biphasic shock the modified action potential wavefront is unable to sustain propagation and fails, whereas following the monophasic shock, action potential propagation is slowed slightly but not halted. Also, in this case, the effect on j is more significant than in the case shown for the single cell. During

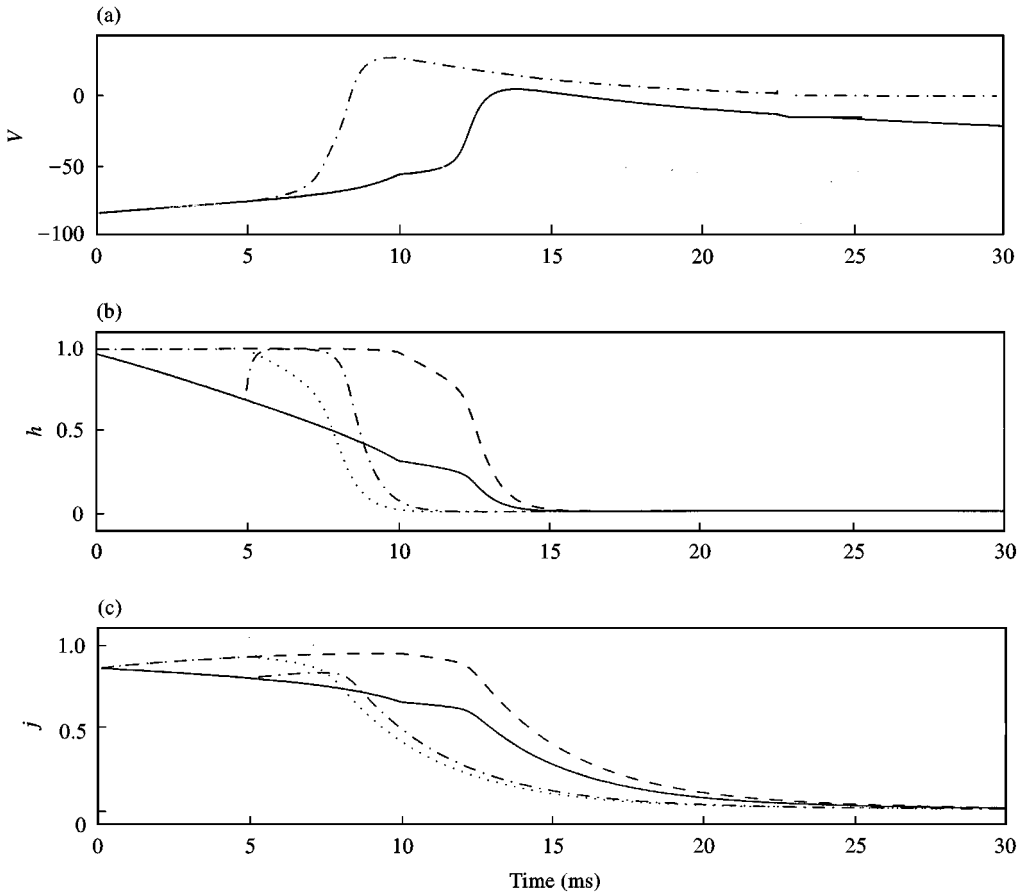

FIG. 8. The transmembrane potential V (in mV) and inactivation variables h and j at position $x = 7.785$ cm on a periodic ring described in the previous figures. The monophasic shock has little effect on the action potential, while the biphasic shock produces direct activation. Notice that the same ionic mechanisms are at work here as in the single cell. The biphasic shock eliminates inactivation in the hyperpolarized portion of the cell with the first phase of the shock, and then activates the cell when the polarity of the shock is reversed. (a) Mono (——); bi (- · · · -). (b) and (c) Mono− (——); mono+ (– – –); bi− (– · – · –); bi+ (·····).

the first half of the pulse at $x = 9.450$ cm, j increases from below 0.5 to above 0.7, whereas there is little change in h.

The effectiveness of monophasic and biphasic shocks for annihilating spiral wave reentry was also studied in two-dimensional collections of cells. For this portion of the study, we used a modified Beeler–Reuter model with the time constants of calcium current activation and inactivation (d and f) halved (Courtemanche & Winfree, 1991). The change in time constants allows the formation of a stable spiral wave on a computationally reasonable domain (10 cm × 10 cm). This stable spiral wave is used as the initial conditions for simulations where external shocks are given. Parameters are the same as for the ring simulations, however for the two-dimensional simulations, the Euler integration method was used with a time-step of 0.025 ms and a space-step of 0.025 cm (Courtemanche & Winfree, 1991; Xu & Guevara, 1998).

Figures 10 and 11 show the membrane potential during and following the application of a monophasic stimulus and a biphasic stimulus, respectively. The stimuli were both of duration 10 ms and amplitude $A = 17.5$. We see that the results here are similar to those for the ring dynamics. The monophasic stimulus pushes the wavefront of the spiral wave forward; however it only manages to shift the phase of the spiral wave and is unable to annihilate it. The biphasic stimulus, on the other hand, is able to push the wavefront of the spiral wave much further into its waveback and activate more of the core than the

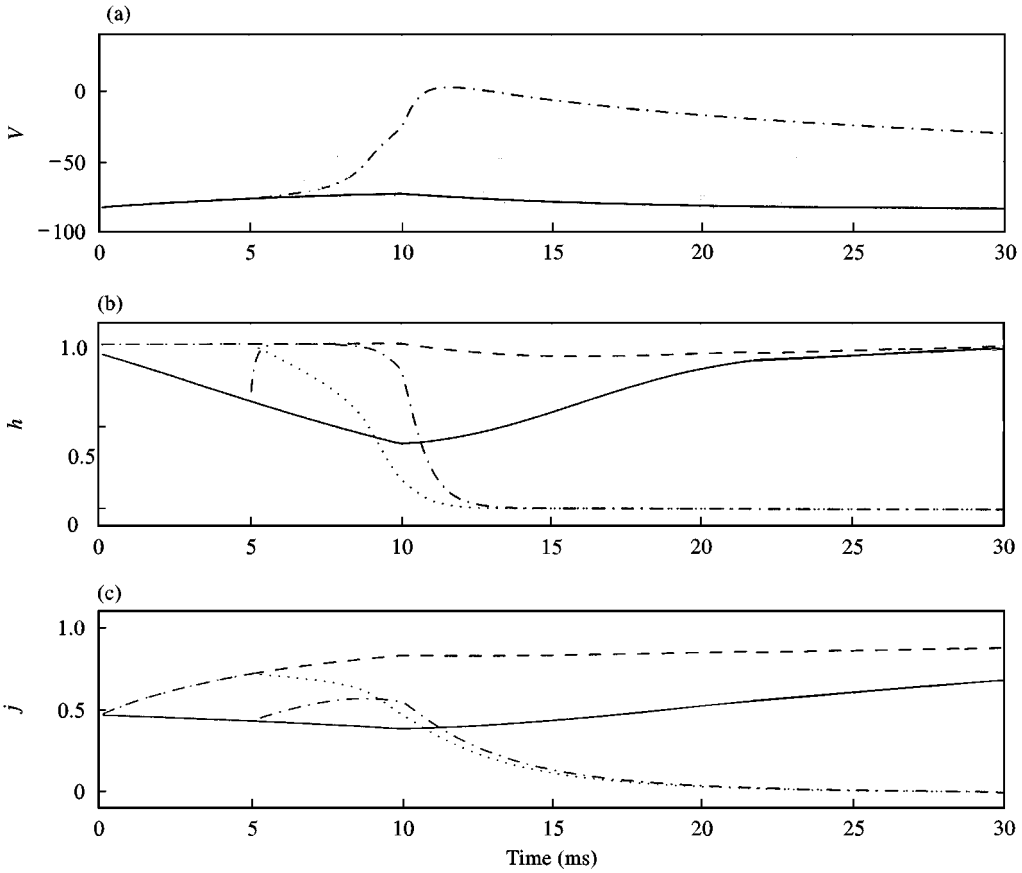

FIG. 9. The transmembrane potential V (in mV) and inactivation variables h and j at position $x = 9.450$ cm on a periodic ring described in the previous figures. Here, the difference between monophasic and biphasic stimuli can be seen even better than in the previous figure. The monophasic shock has almost no effect on the action potential, while the biphasic shock produces direct activation. Notice that the same ionic mechanisms are at work here as in the single cell. The biphasic shock eliminates inactivation in the hyperpolarized portion of the cell with the first phase of the shock, and then activates the cell when the polarity of the shock is reversed. The major facillatory effect of the initial phase of the biphasic stimulus is on j. (a) Mono (——); bi (- · - · -). (b) and (c) Mono− (——); mono+ (– – –); bi− (– · – · –); bi+ (·····).

monophasic stimulus. This is seen best by comparing the $t = 10$ ms panels of Figs 10 and 11. The ionic mechanism responsible for the success here appears to be identical to that described in the cases of the single cell and ring dynamics (not shown).

5. Discussion

There is a substantial difference in the response of ionic models between monophasic and biphasic shocks. This difference occurs because of the relatively fast response time of the sodium inactivation variables. The fundamental mechanism for this difference is that the hyperpolarization phase of the biphasic pulse acts as a pre-pulse to remove inactivation from the cell, accelerating its recovery, and thereby lowering the activation threshold prior to the subsequent polarity reversal.

This mechanism is robust, meaning that it can be observed in a variety of ionic models under varying conditions and parameter values. However, the quantitative details of this phenomenon can vary greatly depending on the detailed structure of the sodium channel and its associated time constants of inactivation. In fact, we have observed as great as a three-fold difference in activation threshold for a particular modification to the Beeler–Reuter model (in which j_∞ was increased) between biphasic and monophasic stimulus protocols. The latest model for sodium inactivation is yet to be incorporated into a full ionic model (Richmond *et al.*, 1998). It should

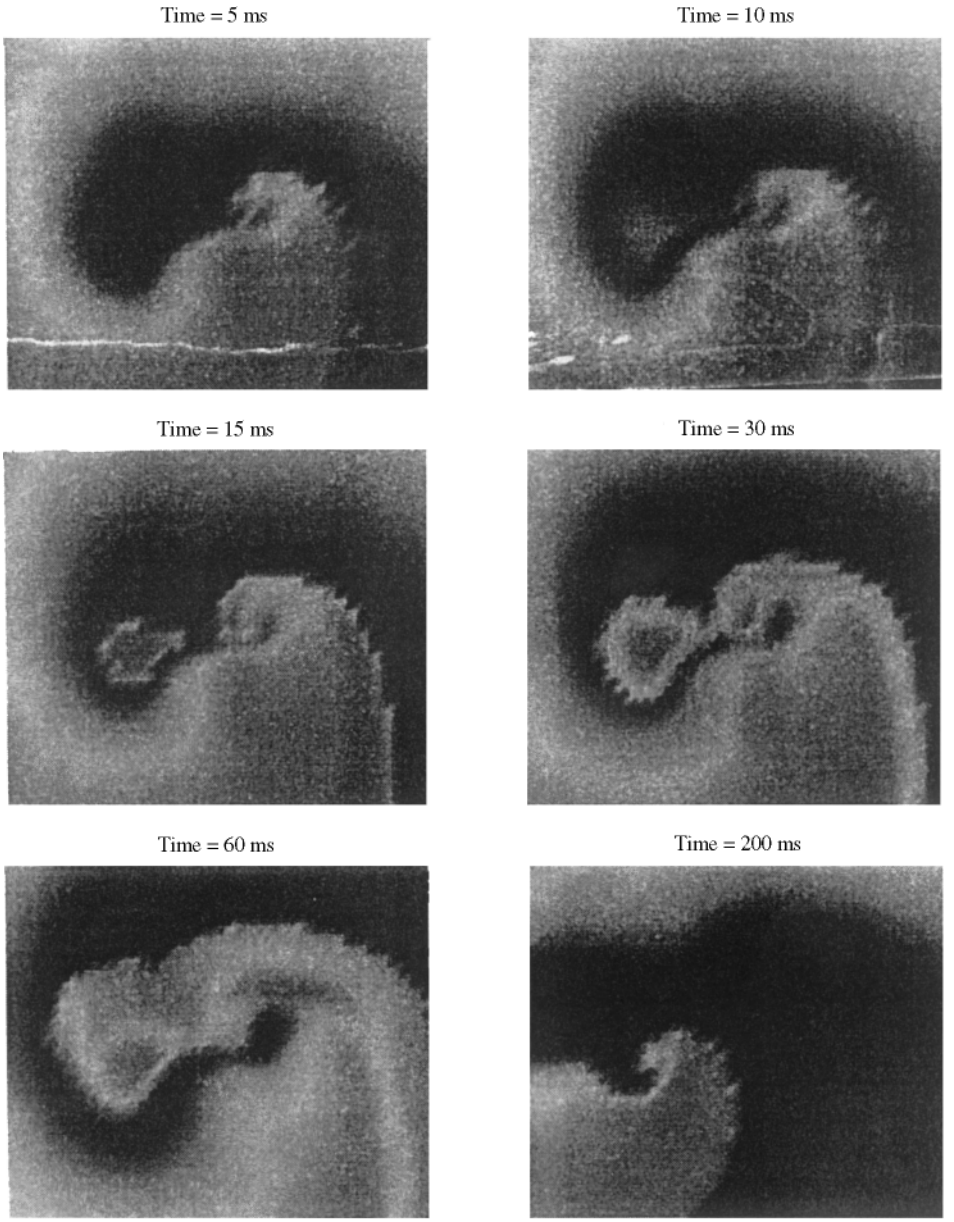

FIG. 10. The transmembrane potential V in a two-dimensional sheet of modified Beeler–Reuter tissue during and following the application of a monophasic stimulus of duration 10 ms and amplitude $A = 17.5$. Prestimulus dynamics correspond to a spiral wave. The monophasic stimulus shifts the phase of the spiral wave, but is unable to annihilate it.

also be noted that the quantitative details involved in determining both monophasic and biphasic activation thresholds depend greatly on currents responsible for recovery as well as excitation currents. A complete quantitative study of defibrillation thresholds, therefore, must include a detailed comparison of different ionic models.

There are several other concerns relating to the quantitative reliability of these results. Specifically, there is need for a convergence study to determine the dependence of these results on the number of cellular compartments. As noted above, different sample numbers have been used to discretize single cells [2 points here, 3 points in Tung & Borderies (1992), 4 points per cell in Fishler *et al.* (1996b), 11 points in Fishler *et al.* (1996b) and 48 points in Leon & Roberge (1993)], although the qualitative results are identical in all of these studies.

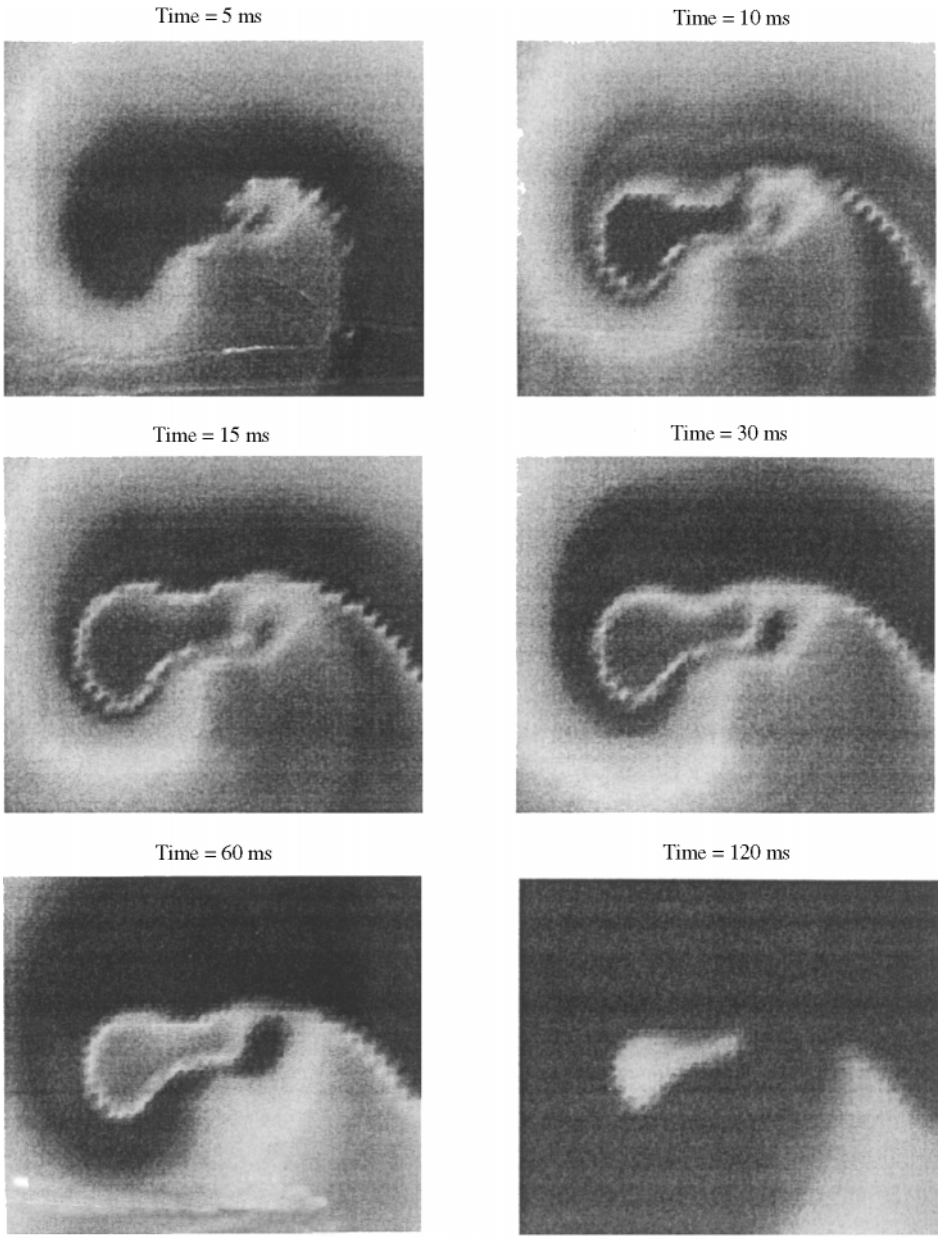

FIG. 11. The transmembrane potential V in a two-dimensional sheet of modified Beeler–Reuter tissue during and following the application of a biphasic stimulus of duration 10 ms and amplitude $A = 17.5$. Prestimulus dynamics correspond to a spiral wave (as in the previous figure). Unlike the monophasic stimulus of the same amplitude and duration, the biphasic stimulus is able to annihilate the spiral wave.

We also do not currently know how to accurately relate the stimulus threshold at the cellular level to tissue level thresholds (although rough estimates give reasonable agreement with experimental results (Keener, 1996, 1998). This is because the functions W_i and W_e, which give a measure of small scale resistive inhomogeneities, are not known. In fact, to date, attempts to directly observe the "sawtooth" potential have failed (Gillis *et al*., 1996; Zhou *et al*., 1998) leading some investigators to dispute the validity of this model. It should be noted, however, that there is no doubt that resistive inhomogeneities play an important role in the distribution of transmembrane currents during a stimulus (Fishler, 1998; Fishler & Vepa, 1998; White *et al*., 1998), nor can one dispute the existence of small-scale resistive inhomogeneities, only whether or not the effect of

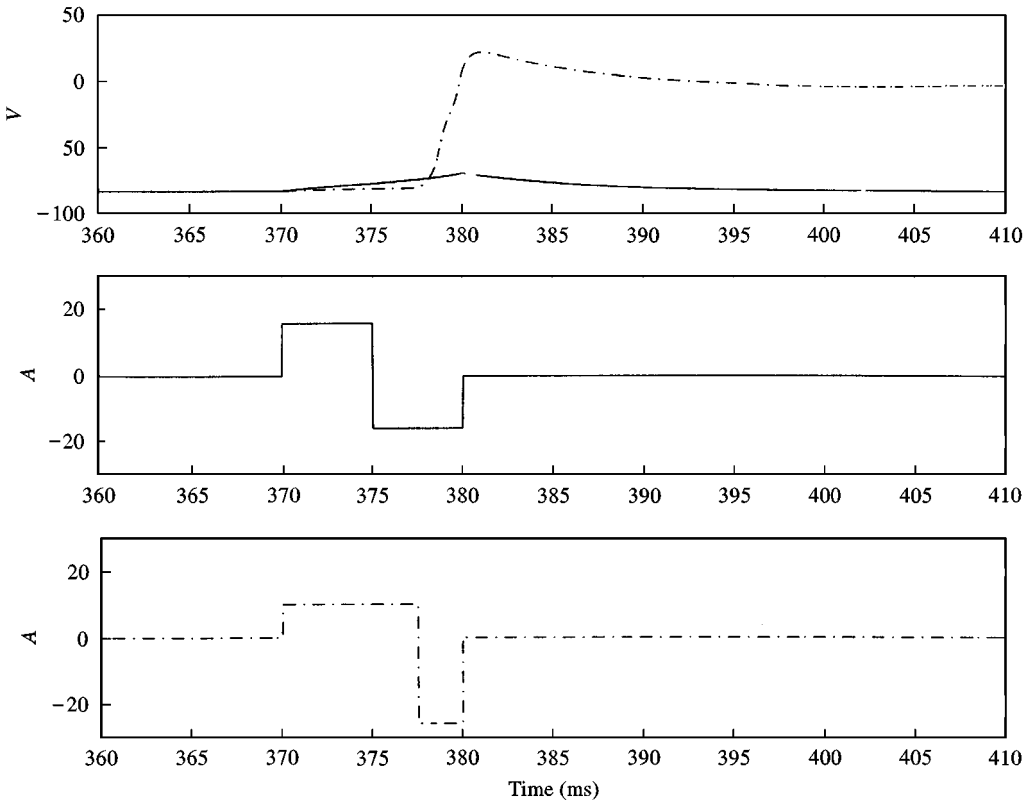

FIG. 12. The transmembrane potential V (mV) of a single cell (top) in respose to the application of two different biphasic stimuli of equal energy and duration (shown in the bottom two traces). The non-symmetric biphasic stimulus is successful in activating the cell, whereas the symmetric one is not. This suggests that there are even more effective stimulus protocols for defibrillation than a symmetric biphasic shock. Stimulus 1 (——); stimulus 2 (– · – · –).

these is sufficient to affect transmembrane current flow at defibrillation strength current levels. There are also numerous technical difficulties with directly observing the sawtooth potential, so that we do not view the current experimental mismatch as definitive or fatal to this theory.

There are other features of defibrillation that this theory does not explain. For example, Strickberger *et al.* (1994) reported a difference in defibrillation threshold between anodal and cathodal monophasic shocks during transvenous defibrillation. The model presented here is symmetrical with respect to the direction of current flow. Termination of ventricular tachycardia is generally considered to require less energy than termination of ventricular fibrillation (AMA Standards, 1986). There is currently no theoretical explanation of this difference.

The obvious question that remains is to determine the optimal biphasic protocol. It is certain that the 50–50 temporal split of polarity phases is not optimal, since there is no symmetry that would demand this. Figure 12 shows the results of two biphasic stimuli with identical total energy (squared area $= 2560\ \text{mV}^2\ \text{ms}$) and duration (10 ms) but with differing consequences. The biphasic pulse with a 50–50 temporal split between phases and equal amplitude ($A = 16$) in the two phases is unsuccessful at evoking a stimulus, while a biphasic stimulus with unequal amplitudes ($A_1 = 10$, $A_2 = 26.46$) and unequal durations ($t_1 = 7.5$ ms, $t_2 = 2.5$ ms) is successful. Thus, there are ways to redistribute the energy that improve the likelihood of successful defibrillation.

Most defibrillators used clinically use truncated exponential waveforms rather than the square waveform used here. The optimal waveform, whether square or a truncated exponential, and its biphasic distribution, is not yet known, although the results presented here provide a way to search for the optimal waveform.

This research was supported in part by NSF Grant DMS 9626334.

REFERENCES

AMA STANDARDS (1986). American Heart Association standards and guidelines for cardiopulmonary resuscitation and emergency cardiac care. *JAMA* **255,** 2841–3044.

BEELER, G. W. & REUTER, H. (1977) Reconstruction of the action potential of myocardial fibres. *J. Physiol* (*Lond.*) **268,** 177–210.

BIKTASHEV, V. & HOLDEN, A. (1998). Re-entrant waves and their elimination in a model of mammalian ventricular tissue. *Chaos* **8,** 48–56.

BIKTASHEV, V., HOLDEN, A. & ZHANG, H. (1997). A model for the action potential of external current onto excitable tissue. *Int. J. Bif. Chaos* **17**.

COURTEMANCHE, M. and WINFREE, A. T. (1991). Re-entrant rotating waves in a Beeler-Reuter-based model of 2-dimensional cardiac electrical activity. *Int. J. Bif. & Chaos* **1,** 431–444.

EBIHARA, L. & JOHNSON, E. A. (1980). Fast sodium current in cardiac muscle, a quantitative description. *Biophys. J.* **32,** 779–790.

FISHLER, M. G. (1998). Synctial heterogeneity as a mechanism underlying cardiac far-field stimulation during defibrillation-level shocks. *J. Cardiovascular Electrophysiology* **9,** 384–394.

FISHLER, M. G., SOBIE, A. A., TUNG, L. & THAKOR, N. V. (1996a). Cardiac responses to premature monophasic and biphasic field stimuli. *J. Electrocardiol.* **28,** 174–179.

FISHLER, M. G., SOBIE, A. A., TUNG, L. and THAKOR, N. V. (1996b). 'Modeling the interaction between propagating cardiac waves and monophasic and biphasic field stimuli: the importance of the induced spatial excitatory response. *J. Cardiovasc. Electrophysiol.* **7,** 1183–1196.

FISHLER, M. G. & VEPA, K. (1998). Spatiotemporal effects of syncytial heterogeneities on cardiac far-field excitations during monophasic and biphasic shocks. *J. Cardiovasc. Electrophysiol.* **9,** 1310–1324.

GILLIS, A. M., FAST, V. G., ROHR, S. & KLEBER, A. G. (1996). Spatial changes in transmembrane potential during extracellular electric shocks in cultured monolayer of neonatal rat ventricular myocytes. *Circ. Res.* **79,** 676–690.

HINES, M. (1984). Efficient computation of branched nerve equations. *Int. J. Biomed. Comput.* **15,** 69–76.

HOLDEN, A. (1997). Defibrillation in models of cardiac muscle. *J. Theor. Med.* **1,** 91–102.

JONES, J. L., JONES, R. E. & BALASKY, G. (1987). Improved cardiac cell excitation with symmetrical biphasic defibrillator waveforms. *Am. J. Phys.* **253,** H1418–H1424.

JONES, J. L., JONES, R. E. & MILNE, K. B. (1994). Refractory period prolongation by biphasic defibrillator waveforms is associated with enhanced sodium current in a computer model of the ventricular action potential. *IEEE Trans. Biomed. Engng* **41,** 60–68.

KEENER, J. P. (1988). *Principles of Applied Mathematics*: *Transformation and Approximation.* Reading, MA. Addison-Wesley.

KEENER, J. P. (1996). Direct activation and defibrillation of cardiac tissue. *J. theor. Biol.* **178,** 313–324.

KEENER, J. P. (1998). The effect of gap junctional distribution on defibrillation. *Chaos* **8,** 175–187.

KEENER, J. P. & PANFILOV, A. V. (1996). A biophysical model for defibrillation of cardiac tissue. *Biophys. J.* **71,** 1335–1345.

KEENER, J. P. & SNEYD, J. (1998). *Mathematical Physiology*. New York: Springer.

KNISELY, S. B., BLITCHINGTON, T. F., HILL, B. C., GRANT, A. O., SMITH, W. M., PILKINGTON, T. C. & IDEKER, R. E. (1993). Optical measurements of transmembrane potential changes during electrical field stimulation of ventricular cells. *Circ. Res.* **72,** 255–270.

KRINSKY, V. I. & PUMIR, A. (1998). Models of defibrillation of cardiac tissue. *Chaos* **8,** 188–203.

LEON, L. J. & ROBERGE, F. A. (1993). A model study of extracellular stimulation of cardiac cells. *IEEE Trans. Biomed. Engng* **40,** 1307–1319.

LUO, C. H. & RUDY, Y. (1994a). A dynamic model of the cardiac ventricular action potential; I: Simulations of ionic currents and concentration changes. *Circ. Res.* **74,** 1071–1096.

LUO, C. H. & RUDY, Y. (1994b). A dynamic model of the cardiac ventricular action potential; II: afterdepolarizations, triggered activity and potentiation. *Circ. Res.* **74,** 1097–1113.

PLONSEY, R. (1988). The use of a bidomain model for the study of excitable media. In: *Some Mathematical Questions in Biology*: *The Dynamics of Excitable Media*, (Othmer, H., ed.), pp. 123–149. RI: AMS.

PUMIR, A. & KRINSKY, V. I. (1996). How does an electric field defibrillate cardiac muscle? *Phys. D* **91,** 205–219.

PUMIR, A. & KRINSKY, V. I. (1997). Two biophysical mechanisms of defibrillation of cardiac tissue. *J. theor. Biol.* **185,** 189–199.

PUMIR, A., ROMEY, G. & KRINSKY, V. I. (1998). De-excitation of cardiac cells. *Biophys. J.* **74,** 2850–2861.

RICHMOND, J. E., FEATHERSTONE, D. E., HARTMAN, H. A. & RUBEN, P. C. (1998). Slow inactivation in human cardiac sodium channels. *Biophys. J.* **74,** 2945–2952.

STRICKBERGER, S. A., HUMMEL, J. D., HORWOOD, L. E., JENTZER, J., DAOUD, E., NIEBAUER, M., BAKR, O., MAN, K. C., WILLIAMSON, B. D., KOU, W. & MORADY, F. (1994). Effect of shock polarity on ventricular defibrillation threshold using a transvenous lead system. *J. Am. Coll. Cardiol.* **24,** 1069–1072.

TUNG, L. & BORDERIES, J.-R. (1992). Analysis of electric field stimulation of single cardiac muscle cells. *Biophys. J.* **63,** 371–386.

WHITE, J. B., WALCOTT, G. P., POLLARD, A. E. & IDEKER, R. E. (1998). Myocardial discontinuities: a substrate for producing virtual electrodes that directly excite the myocardium by shocks. *Circulation* **97,** 1738–1745.

XU, A. & GUEVARA, M. R. (1998). Two forms of spiral-wave reentry in an ionic model of ischemic ventricular myocardium. *Chaos* **8,** 157–174.

ZHOU, X., DAUBERT, J. P., WOLF, P. D., SMITH, W. E. & IDEKER, R. E. (1993a). Epicardial mapping of ventricular defibrillation with monophasic and biphasic shocks in dogs. *Circ. Res.* **72,** 145–160.

ZHOU, X., KNISELY, S. B., SMITH, W. M., ROLLINS, D., POLLARD, A. E. & IDEKER, R. E. (1998). Spatial changes in the transmembrane potential during extracellular electric stimulation. *Circ. Res.* **83,** 1003–1014.

ZHOU, X., WOLF, P. D., ROLLINS, D. L., AFEWORK, Y., SMITH, W. E. & IDEKER, R. E. (1993b). Effects of monophasic and biphasic shocks on action potentials during ventricular fibrillation in dogs. *Circ. Res.* **73,** 325–334.